Engineering and Technology Journal
Journal homepage: https://etj.uotechnology.edu.iq

Characterization of the Efficiency of Photo-Catalytic Ultrafiltation PES Membrane Modified with Tungsten Oxide in the Removal of Tinzaparin Sodium

Reham R. Abdullah[a], **Kadhum M. Shabeeb**[a], **Aseel B. Alzubaydi** [a], **Alberto Figoli** [b], **Alessandra Criscuoli** [b], **Enrico Drioli** [b], **Qusay F. Alsalhy**[*c]

[a]Materials Engineering Dept, University of Technology-Iraq, Alsina'a Street, 10066 Baghdad, Iraq.
[b] Institute on Membrane Technology, National Research Council (ITM-CNR), 87030 Rende, CS, Italy.
[c] Membrane Technology Research Unit, Chemical Engineering Dept, University of Technology-Iraq, Alsina'a Street, 10066 Baghdad, Iraq.
*Corresponding author Email: qusay.f.abdulhameed@uotechnology.edu.iq

HIGHLIGHTS

- Preparation of tungsten oxide ($WO_{2.89}$) NPs immobilized PES matrix.
- Antifouling performance was evaluated against tinzaparin sodium.
- Further enhancement was noticed after exposing the membranes to UV irradiation.

ARTICLE INFO

Handling editor: Mustafa H. Al-Furaiji
Keywords:
ultrafiltration
photocatalytic membranes
tungsten oxide
tinzaparin sodium
antifouling
wastewater treatment

ABSTRACT

One of the polymeric membranes' main limitations is their susceptibility to fouling, lowering the membrane's performance with time. Therefore, incorporating nanomaterials in polymer matrices has attracted great attention in wastewater treatment applications. It's a promising approach for enhancing membrane hydrophilicity and performance. Herein, ultrafiltration nanocomposite membranes were synthesized by applying the phase inversion method through immobilizing (0.1-0.4 wt.%) tungsten oxide ($WO_{2.89}$) nanoparticles in a polyether sulfone (PES) matrix. Membrane's anti-fouling performance was evaluated against tinzaparin sodium. The data showed that the pure water flux improved with increasing nanoparticle loading, reaching its optimum value of 54.9 kg/m^2 h at 0.4 wt.% $WO_{2.89}$ nanoparticles compared to the neat membrane's 30.42 kg/m2 h. The results also demonstrated that the rejection efficiency and flux recovery ratio (FRR) against tinzaparin sodium was enhanced, by 44.89% and 12.69%, respectively, for the membranes modified with 0.4wt.% $WO_{2.89}$ nanoparticles loading compared to the neat PES membrane. The data also showed that after exposing the nanocomposite membranes to UV light irradiation (λ=365 nm) and intensity (1200mW/cm^2) for 1h, a further enhancement by 8.34% in FRR as compared to the membranes with the same percentage of nanoparticles loading without irradiation. It is concluded that the photocatalytic activity of $WO_{2.89}$ nanoparticles in the decomposition of organic molecules on/close to the membrane surface was the impact that caused this improvement in membrane anti-fouling property.

1. Introduction

With the rapid development of industry, larger amounts of wastewater are being produced, causing damaging effects on the safety of usable water. Recently, membrane techniques have been taking a crucial role in water purification [1]. They have been used extensively in various sectors, including wastewater treatment, water desalination, food, pharmaceutical, chemical, biological, petrochemical processes, and many others. These techniques have proven to be a reliable and excellent alternative to conventional treatment techniques in wastewater treatment [2-5]. They offer environmental safety, high separation efficiency, low energy consumption, and easy maintenance compared to other conventional separation processes making them an outstanding option for wastewater treatment, operating either alone or within a hybrid process [6-8]. Although membrane techniques play an important role in wastewater treatment, fouling still limits their use in many applications. Due to the

http://doi.org/10.30684/etj.2022.134070.1219
Received 31 May 2022; Accepted 26 June 2022; Available online 10 August 2022

.

adsorption of organic pollutants, fouling reduces water transport across the membrane and deteriorates other functional properties of the membrane surfaces, increasing energy consumption and shortening membrane life [9, 10].

The tradeoff between selectivity and permeability is another challenge. Enhancing one without compromising the other for the currently used polymeric membranes is difficult. Integrating nanoparticles with polymeric matrices anticipates that polymeric membranes can benefit from nanoparticles' superior properties to cope with some weaknesses, such as their propensity for fouling [11]. Membranes performance and separation properties were found be to enhanced with incorporating nanoparticles in/on polymeric matrices, such as zinc sulfide (ZnS) [12], titanium dioxide (TiO_2) [13], zinc oxide (ZnO) [14, 15], graphene oxide (GO)[16], carbon nanotube (CNTs), magnesium oxide (MgO), silicon dioxide (SiO_2)[17], MWCNTs, iron(III) oxide (Fe_2O_3), and graphene oxide-silica (GO/SiO_2) [18-21]. In recent years, photocatalytic membranes have drawn great attention in water treatment due to their superior characteristics (e.g., anti-fouling and improved permeate quality). Nowadays, photocatalytic technology has become one of the greens and most efficient processes for eliminating hazardous pollutants in wastewater treatment. It is a green and environment-friendly process for contaminants removal [22, 23, 2]. The membrane has been functionalized by incorporating nanoparticles deposited on the surface or embedded into the matrices to result in tailored properties such as the ability to bind specific contaminants or catalyze degradation reactions. Membranes could perform the role of a supporting matrix for the photocatalyst. If a proper membrane is used, it will function as a selective barrier for the species to be degraded. Semiconductor nanoparticles are quite effective in wastewater purification. Some examples of semiconductor nanoparticles are ZnO, ZnS, gallium nitride (GaN), gallium phosphide (GaP), cadmium sulfide (CdS), cadmium selenide (CdSe), and cerium fluoride (CeF_3) [21, 24-28]. Among these extraordinary photocatalytic nanomaterials are those made of WO_3, which reported a stupendous performance as photocatalysts, gas sensors, and electrochromic devices. WO_x x $\leq$3 nanomaterials have gained considerable attention as a result of their abundance, high oxidation ability, and chemical stability at suitable pH values [29, 30]. They are n-type semiconductors with band-gap energy between 2.4–3.0 eV [31, 32]. WO_3 is also recognized for its nonstoichiometric properties, as the lattice can hold a considerable number of oxygen vacancies (WO_3, $WO_{2.9}$, $WO_{2.8}$, $WO_{2.72}$, and WO_2). Since photocatalytic activity is fundamentally influenced by the recombination rate of the photo-generated electrons and holes, many attempts have been made to minimize such limitations and enhance the separation and migration of these photo-generated holes and electrons [29, 30, 33, 34]. Mohd Hir et al. (2017) [35] immobilized photocatalytic nanoparticles (ZnO) into a PES matrix. The photoactivity of the modified membranes increased in the degradation of methyl orange dye. Sing et al. [8] noticed that the removal of ibuprofen (IBP) was increased in the PSF membrane modified with copper oxide (Cu_2O) photocatalyst under irradiation. Hydrophilicity and anti-fouling properties were higher for the modified membranes. Zakeritabar et al. (2020) reported that the degradation efficiency of pharmaceutical contaminants revealed a greater rejection of the PSF/ CeF_3 membranes under UV radiation than the neat PSF membrane. PSF/CeF_3-0.75% membrane had a rejection value of higher than 97%, and COD removal was higher than 65%, while they were 75% and 31%, respectively, for the neat PSF membrane [28].

Pharmaceutical residues released into the environment are a growing concern because of the significant effects on humans, animals, and microbial communities. Pharmaceuticals can be only partly metabolized during therapeutic use, releasing residual fractions into the sewer [36]. These residues have complex composition, with elevated concentrations of organic matter and salt and high microbial toxicity. They are also hard to bio-degrade, which causes damage to the environment and requires their removal [37]. Pharmaceuticals' presence in water comes from two sources: pharmaceutical industries and human utilization of these compounds. Approximately half of the produced pharmaceutical wastewaters worldwide are discarded worldwide without specific treatment [38]. In this work, nanocomposite ultrafiltration membranes were synthesized of PES matrix modified with $WO_{2.89}$ nanoparticles at different concentrations. Tinzaparin sodium was used as a simulated fouled molecule with molecular weight (approximately 6,500 Da) to test the anti-fouling property of the membranes. It was not considered an actual pollutant.

2. Materials and Methods

2.1 Materials

Polyethersulfone (PES, Ultrason E6020P) was donated as a polymer by BASF, Germany. Polyvinylpyrrolidone (PVP) (40 kDa), as a pore-forming agent, and Dimethyl sulfoxide (DMSO), as a solvent, were both purchased from Central Drug House, India. Tungsten Oxide $WO_{2.89}$ (W_{19} O_{55}), with an average particle size of 80-100 nm and purity of 99.9%, was obtained from Hongwu International Group Ltd. Tinzaparin sodium (anti-thrombotic drug) was obtained from LEO Pharma, with a molecular weight of approximately 6500 daltons, and used to evaluate the anti-fouling property of the membranes. The composition of tinzaparin sodium injection is tinzaparin sodium, benzyl alcohol, sodium metabisulfite, sodium hydroxide, and water. The bioavailability of tinzaparin ranges from 30% to 70% [39, 40].

2.2 Membrane Preparation

The nonsolvent induced phase separation method synthesized all neat, and WO2.89 NPs modified membranes. An appropriate amount of PES polymer was initially dried at 60°C for 4h to eliminate the moisture content. Fixed amounts of 19 wt.% PES and 1wt.% PVP were dissolved in 80 wt.% DMSO solvent and stirred at room temperature using magnetic stirring until a homogenous solution is achieved. A certain amount of $WO_{2.89}$ NPs was added to the mixture and stirred for another 4h, followed by sonication using KQ32OOE Ultrasonic device at 200 rpm for 30 min with 40 kHz operating frequency at room temperature. The applied ultrasonic power was 150W to obtain a homogenous dispersion. The content of the nano additives in the mixture was varied (0.1, 0.2, 0.3, and 0.4 wt.%). The solution was then cast on a glass substrate with 200-micron clearance

gab via an automatic film applicator. The resultant film was immersed in a coagulation water bath at 30°C, and the humidity was 32%. Finally, the prepared membranes were rinsed thoroughly and kept in DI water for 24 hours to remove any solvent residuals. The membranes were then stored in 30wt.% glycerol solution ready for further characterization [16]. Pure water flux of the membranes was measured at higher NPs loading. In contrast, a lower flux value was observed even less than the control membrane. Thereby higher NPs loading wasn't used in the current work.

2.3 Characterization of Membranes

In the previous research, characterizations of the membranes were studied [41]. Cross section images were obtained from SEM. It was found that the finger-like pores started to widen and elongate along the membranes' cross-section with increasing NPs loading membrane. Also, roughness and mean pore size values were obtained from AFM. The data showed that the roughness value decreased from 36.5 nm at the control membrane to 12 nm at 0.4 wt.% NPs loading membrane. Additionally, the membrane's mean pore size decreased from 107.7 nm at the control membrane to 74.4 nm at 0.4 wt.% NPs loading membrane. The contact angle values of the membranes decreased with NPs addition, and the optimum value was 51.216˚ at 0.4wt.% NPs loading compared to the neat membrane, which exhibited about 68.179%. The porosity of the synthesized membranes showed an enhanced value (64.2%) with the highest NPs loading ratio (0.4 wt.%). The maximum tensile strength value was recorded at 0.4 wt.% nanocomposite membrane. The results are presented in Table 1.

2.4 Membranes Performance

2.4.1 Pure water flux

The performance of the membranes was measured using a cross-flow (CF) filtration system that was assembled manually. The system comprises a cross-flow acrylic cell, two pressure gauges, a flow meter, a feed tank, a pump (model No.AQ-75GPD), and a digital scale to measure permeate weight, as shown in Figure 1A. The testing was performed at 5 bar and room temperature, and DI water was used throughout all the experiments. Pure water flux (PWF) was calculated as given in the following equation [42]:

$$J = \frac{W}{t \times A} \quad (1)$$

J is the pure water flux of the membrane (kg/h m^2), W is the permeate flux weight (kg), t is the experiment time (h), and A is the active membrane area (m^2). The cell was purchased from Sterlitech Company (CF016 module) with an active membrane area of 20.6 cm^2, maximum operating pressure of 27.6 bar, and a maximum operating temperature of 88 ˚C. The membrane rejection was calculated using the following equation [20]:

$$\text{Rejection}\% = \frac{C_f - C_p}{C_f} \times 100\ \% \quad (2)$$

where C_f and C_p represent the concentration of the feed and permeate (mg/L), respectively. To assess the anti-fouling characteristics of the prepared membranes, the samples were placed in a container inside a dark chamber and covered by an aluminum foil to prevent light interference. They were subjected to 100W UV light (λ=365 nm) and intensity (1200mW/cm^2) for 1h. Figure 1B shows the membranes before and after irradiation. Then, the membrane flux was recorded again. Flux recovery ratio (FRR) was calculated, as given by equation (3) [43], to assess the membranes' anti-fouling performance. J_2 and J_1 represent pure water flux of fouled and cleaned membranes, respectively.

$$FRR = \frac{J_2}{J_1} \times 100\% \quad (3)$$

Table 1: Neat and modified membranes characteristics

NPs wt.%	Roughness (nm)	Mean pore size (nm)	Contact angle(˚)	Porosity (%)	Tensile strength MPa
0	36.5	107.7	68.179	44.9	0.82
0.1	40	98.6	63.33475	58.7	0.833
0.2	21	92.6	61.785	60	1.6
0.3	23	75.5	61.583	62.5	1.663
0.4	12	74.4	51.21675	64.2	1.675

2.4.2 Membranes' performance against tinzaparin sodium

The cross-flow filtration system was used to measure membrane performance against tinzaparin sodium. The testing was performed at 5 bar and room temperature. Membrane flux was calculated using equation (1). Membrane performance was evaluated through stages. After measuring pure water flux, tinzaparin sodium was added to the feed, fed into the filtration system, and flux was measured for 30 minutes. To evaluate anti-fouling performance, the fouled membranes were exposed to UV light for 1 hour, and flux was recorded for 30 min. The fouled membranes were placed in a container containing DI water inside a dark chamber, as shown in Figure 1B, and covered with aluminum foil to prevent light interference. FRR% was calculated using equation (3).

2.4.3 Membrane rejection against tinzaparin

Membrane rejection was evaluated using a tinzaparin sodium injection with a 1 ml dose of 10000 IU in the feed solution as a simulated pollutant. The initial and final concentrations of tinzaparin were measured using the chemical oxygen demand (COD) test, the Lovibond model. COD test describes the amount of oxygen required to break down pollutants chemically. The inspection was performed at the Environmental Research Center/ University of Technology, Baghdad, Iraq. First, membrane rejection was calculated using equation (2). In this test, the samples were pipetted into vials that contained digestion solution (oxidant (mostly potassium dichromate), sulfuric acid, and metal salts) of COD and were mixed thoroughly for half a minute. Then, the vials were placed into a COD reactor (ET108) and heated at 150 °C. After 120 min, the heater was turned off, and the vials were placed at ambient temperature. The samples were then placed in a spectrophotometer to measure their absorbance. Middle range vials were used, with a detection range of 0-1500 mg/L.

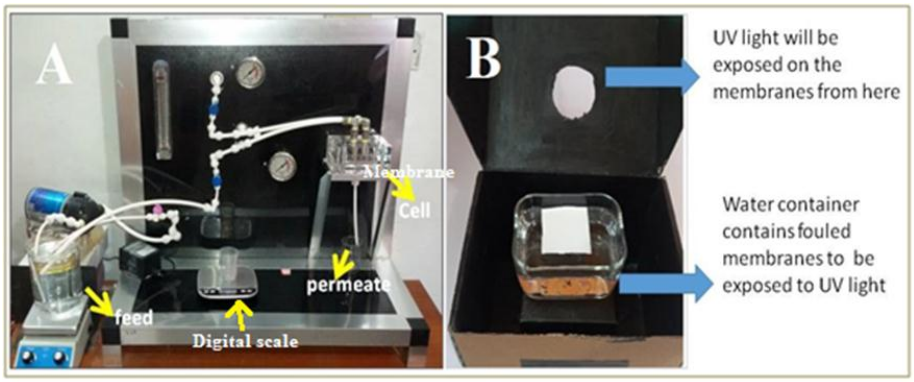

Figure 1: A- Scheme of the UF membrane filtration system; B- Setup of the photocatalytic process

3. Results and Discussion

3.1 Membranes Performance Against Tinzaparin

Figure 2A shows the water flux values of neat and modified membranes at different processes; initial value, after adding tinzaparin sodium to the feed, after cleaning with water, and after UV light irradiation. It was noticed that the addition of $WO_{2.89}$ nanoparticles to the PES membrane matrix improved the water flux of the membranes, reaching its optimum flux value of 54.9 kg/m^{2}h at 0.4 wt.% $WO_{2.89}$ compared to 30.42 kg/m^{2}h of the neat membrane. The enhancement in flux value can be ascribed to the enhancement of the structural properties of the membrane, such as porosity, hydrophilicity, surface roughness, and pore size distribution, as mentioned in previous research [41]. These results agree with earlier investigations [44, 45, 18]. Figure 2A showed that the use of tinzaparin in the filtration system resulted in a reduction in permeate flux. Nevertheless, the membranes modified with the NPs had higher flux than the neat membrane. However, with the addition of $WO_{2.89}$ nanoparticles to the membranes, the flux rate declined from 27.67 % at the neat membrane to about 18.9 % at the 0.4 wt.% nanoparticles modified membrane. This can be explained by the possibility that the presence of $WO_{2.89}$ NPs within the membrane matrix enhanced membrane hydrophilicity and lowered surface roughness, thereby lowering the membrane fouling. These results agree with other authors' reports [46, 47]. The fouled membranes were backwashed with DI water to remove the loosely bonded molecules, after which there was a slight improvement in the flux. Even though SEM and AFM characterizations weren't done to the fouled membrane, the explanation of the presence of fouling on the membrane's surface was based on the observation of flux values after using tinzaparin in the feed. The reduction in flux value when tinzaparin molecules were used in the feed indicated that tinzaparin molecules were deposited on the membrane surface or within the pores during filtration and caused fouling.

Further improvement was observed in flux value after exposing the membranes to UV light irradiation. The improvement in flux was more noticeable at higher nanoparticle loading, as shown in Figure 2B. The optimum flux value was 50.7 kg/h.m^2 at the membrane modified with 0.4 wt.% NPs loading compared to 23.97 kg/h.m^2 at the neat membrane, showing an increment of 111.51%. The enhancement in the flux value can be attributed to the improvements in hydrophilicity and the photocatalytic property of $WO_{2.89}$ NPs. Under irradiation with energy equal to or higher than the band-gap energy of the semiconductor, $WO_{2.89}$ is excited to generate electrons and holes. OH, radicals formed from the redox reaction contribute to removing

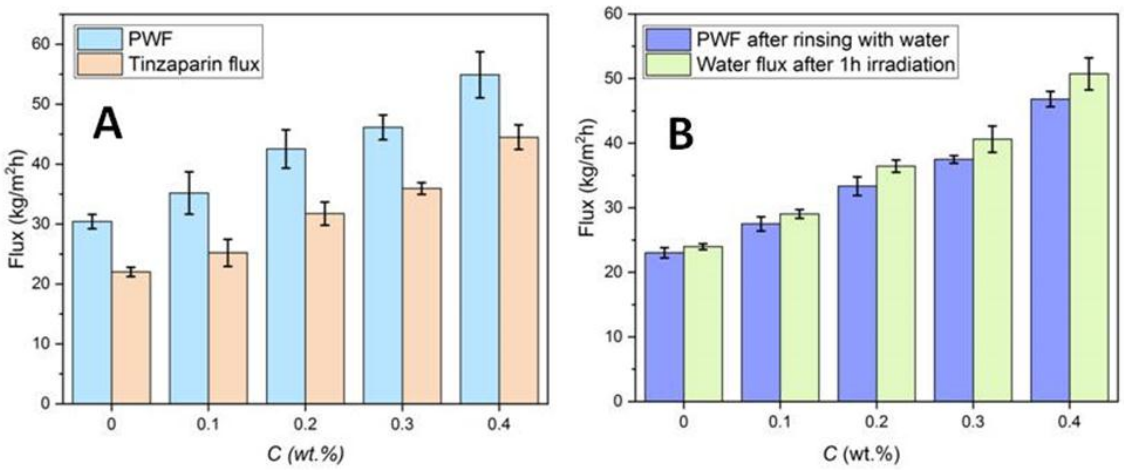

Figure 2: Flux values of neat and modified membranes at different processes; A- Flux with tinzaparin solution in the feed; B- Water flux before/after UV irradiation

tinzaparin and lowering fouling on the membrane surface, thereby enhancing the membrane's flux. These results are consistent with data reported by previous research [48,49]. In addition, the photo-generated electrons can be trapped by the oxygen vacancies in the oxide, reducing the electron-hole recombination effect and enhancing the photocatalytic activity of $WO_{2.89}$ nanoparticles [50]. However, UV light irradiation had a low effect on the neat membrane flux. This implies the low efficiency of the neat membrane in removing tinzaparin without photocatalytic nanoparticles.

3.2 Membrane Rejection Against Tinzaparin

Tinzaparin removal efficiency (R %) values of neat and modified membranes are presented in Figure 3. It was observed that the rejection percentage of the membranes to tinzaparin was enhanced with increasing nanoparticle concentration. In particular, the highest rejection efficiency was obtained with 0.4 wt.% NPs modified membrane, where 71% enhancement was achieved compared to 49% at the neat membrane, which implies 44.89% enhancement. The results can be explained by the enhancement in membrane hydrophilicity due to the presence of nanoparticles that minimized membrane fouling. Another possibility is the reduction in surface roughness and mean surface pore size with increasing NPs loading, which restricts tinzaparin passage through the membrane, thereby increasing the tinzaparin rejection rate. Our results agree with those of earlier investigation [51, 52]

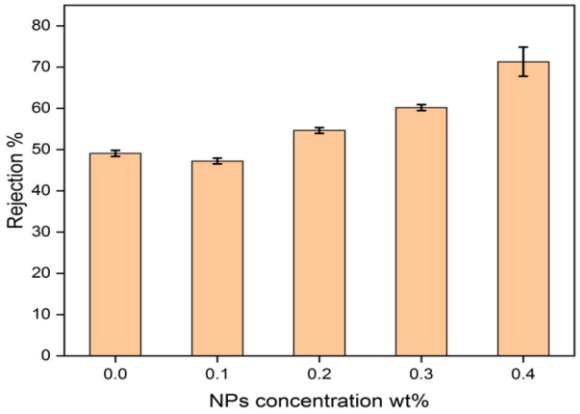

Figure 3: Effects of $WO_{2.89}$ loading on membrane rejection efficiency against tinzaparin sodium

3.3 Flux Recovery Ratio of the Membranes

Figure 4 illustrates the flux recovery ratio (FRR) of the neat and modified membranes without and under UV irradiation. It was noticed that FRR was improved from 75.66% at the neat PES membrane to 85.26% at 0.4 wt.% nanoparticles loading membrane, implying an increment of 12.69%. The results can be explained by the improved surface hydrophilicity of the membranes modified with $WO_{2.89}$ nanoparticles that may lead to the formation of a water molecule layer on the membrane surface, thereby reducing foulants. Besides, membrane fouling was also affected by surface roughness. A smoother surface membrane results in lower fouling, thereby enhancing flux recovery. Therefore, it can be concluded that NPs addition reduced the fouling capacity, which agrees with reports by other groups [44, 53].

Exposing the samples to irradiation has promoted further improvement in FRR, as displayed in Figure 4. The FRR was noticed to increase with nanoparticle loading. The maximum flux value was 92.38 % at the membrane modified with 0.4wt.%

nanoparticles content in comparison to 78.79% at the neat PES membrane. The FRR of the irradiated 0.4 wt.% NPs modified membrane increased by 8.34% compared to the membranes modified with the same percentage of NPs loading without irradiation. This can be explained by the improved photocatalytic activity of $WO_{2.89}$ nanoparticles; reactive radicals generated under irradiation of $WO_{2.89}$ decompose the tinzaparin sodium on the membrane surface, thereby enhancing anti-fouling characteristics of the modified membranes and improving the flux value. These results demonstrate consistency with previously published data [54, 52]. The higher flux values of NPs modified membranes were obtained when clean membranes were used. When fouled membranes were used, the flux value of the fouled membrane exposed to UV light was compared to the flux values without UV light exposure. It was found that the improvement in the flux value was noticeable in the UV light irradiated fouled membrane as compared to flux values of the membranes rinsed with water only 2].

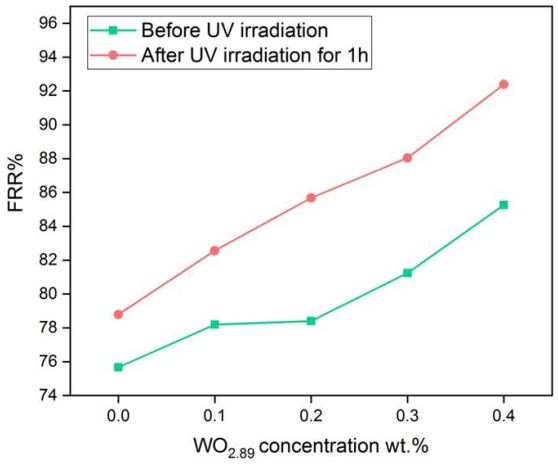

Figure 4: FRR of the neat and modified membranes with and without UV light irradiation

3.4 Proposed Interaction Mechanism

The proposed interaction mechanism between tinzaparin solution and the membrane is shown in Figure 5. Even though membrane and tungsten oxide surface charges were not yet measured, the explanation was based on analyzing the molecules' functional groups and their possible interaction with tinzaparin. It suggests that tinzaparin can be adsorbed on the surface through O-H and N-H bonds. Since both O-H and N-H bonds are partial positive, they are attracted to the partial negative bonds in both polyether sulfone and tungsten oxide, S=O and W=O, respectively. Therefore, during filtration with tinzaparin molecules in the feed solution, the molecules adsorb on the surface, causing a reduction in the flux by blocking some of the pores on the surface and within the membrane. The reduction in flux was noticed to be lower at the modified membranes than at the neat membrane; this was due to the presence of hydrophilic $WO_{2.89}$ nanoparticles that reduced membrane fouling. Also, during the photocatalytic process, the reactive radicals will react with the adsorbed molecules and remove them, enhancing membrane hydrophilicity.

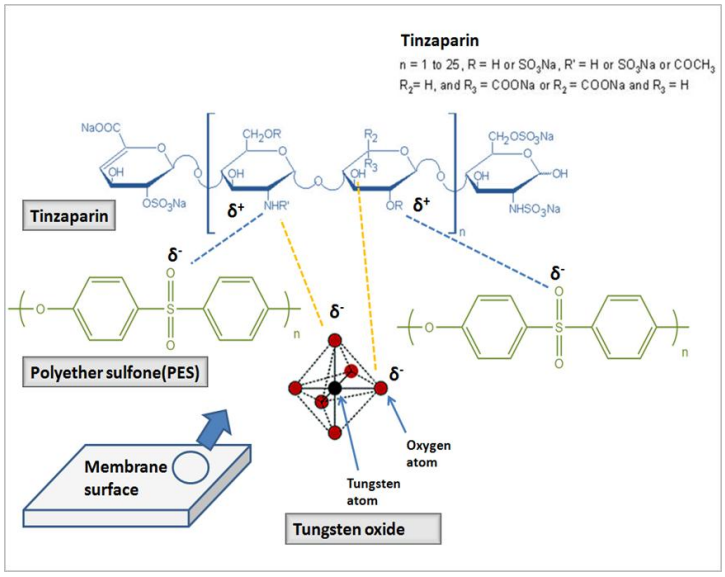

Figure 5: Proposed interaction mechanism of the membranes with tinzaparin

4. Conclusion

In the current study, ultra-filtration nanocomposite membranes were synthesized by modifying the PES matrix with $WO_{2.89}$ nanoparticles. Anti-fouling performance of the membranes was evaluated against tinzaparin sodium. The results showed that the rejection efficiency and FRR of the membrane against tinzaparin were improved for the membrane modified with nanoparticles and reached optimum values of 71% and 85.26%, respectively, at 0.4wt% NPs loading. Furthermore, the nanocomposite-modified membrane had a higher FRR than that of the unmodified membrane after being exposed to irradiation. In particular, the FRR of 0.4 wt.% NPs modified membrane increased by about 8.34% compared to the membrane with the same percentage of NPs loading without irradiation. It is concluded that the photocatalytic activity of $WO_{2.89}$ nanoparticles in the decomposition of organic molecules on/close to the membrane surface was the impact that caused this improvement.

Author contribution

The authors contributed equally to the research.

Correspondences

Correspondences (Qusay F. Alsalhy[1] and Reham R. Abdullah[2]), Engineering and Technology Journal; University of Technology, Baghdad, Iraq; P. O. Box: 35010; Email: qusay.f.abdulhameed@uotechnology.edu.iq[1], mae.20.43@grad.uotechnology.edu.iq[2]

Data Availability Statement

The research is part of my Ph.D. thesis

References

[1] N. Li *et al.*, "Precisely-controlled modification of PVDF membranes with 3D TiO2/ZnO nanolayer: enhanced anti-fouling performance by changing hydrophilicity and photocatalysis under visible light irradiation," *J. Membr. Sci.*, 528 (2017) 359–368. doi: https://doi.org/10.1016/j.memsci.2017.01.048.

[2] H. Bai, X. Zan, L. Zhang, and D. D. Sun, "Multi-functional CNT/ZnO/TiO2 nanocomposite membrane for concurrent filtration and photocatalytic degradation," *Sep. Purif. Technol.*, 156 (2015) 922–930. doi: https://doi.org/10.1016/j.seppur.2015.10.016.

[3] S. Yang, Q. Zou, T. Wang, and L. Zhang, "Effects of GO and MOF@GO on the permeation and antifouling properties of cellulose acetate ultrafiltration membrane," *J. Membr. Sci.*, 569, (2019), 48–59, doi: https://doi.org/10.1016/j.memsci.2018.09.068.

[4] R. J. Kadhim, F. H. Al-Ani, and Q. F. Alsalhy, "MCM-41 mesoporous modified polyethersulfone nanofiltration membranes and their prospects for dyes removal," *Int. J. Environ. Anal. Chem.*, (2021) 1–21. doi: 10.1080/03067319.2020.1865326.

[5] M. Al-Furaiji, K. Kalash, M. Kadhom, and Q. Alsalhy, "Evaluation of polyethersulfone microfiltration membranes embedded with MCM-41 and SBA-15 particles for turbidity removal," *Desalin. Water Treat.*, 215 (2021) 50–59. doi: 10.5004/dwt.2021.26764.

[6] C. Ferreiro *et al.*, "Contaminants of Emerging Concern Removal in an Effluent of Wastewater Treatment Plant under Biological and Continuous Mode Ultrafiltration Treatment," *Sustainability* , 12 (2020) 725. doi: 10.3390/su12020725.

[7] E. Dadvar, R. R. Kalantary, H. Ahmad Panahi, and M. Peyravi, "Efficiency of Polymeric Membrane Graphene Oxide-TiO_2 for Removal of Azo Dye," *J. Chem.*, (2017) 6217987. doi: 10.1155/2017/6217987.

[8] R. Zhang *et al.*, "A novel photocatalytic membrane decorated with PDA/RGO/Ag3PO4 for catalytic dye decomposition," *Colloids Surfaces A Physicochem. Eng. Asp.*, 563 (2019) 68–76. doi: https://doi.org/10.1016/j.colsurfa.2018.11.069.

[9] X. Li *et al.*, "Self-assembly of TiO2 nanoparticles around the pores of PES ultrafiltration membrane for mitigating organic fouling," *J. Membr. Sci.*, 467 (2014) 226–235. doi: https://doi.org/10.1016/j.memsci.2014.05.036.

[10] N. Haghighat, V. Vatanpour, M. Sheydaei, and Z. Nikjavan, "Preparation of a novel polyvinyl chloride (PVC) ultrafiltration membrane modified with Ag/TiO2 nanoparticle with enhanced hydrophilicity and antibacterial activities," *Sep. Purif. Technol.*, 237, (2020), 116374, doi: https://doi.org/10.1016/j.seppur.2019.116374.

[11] Y. Wen, J. Yuan, X. Ma, S. Wang, and Y. Liu, "Polymeric nanocomposite membranes for water treatment: a review," *Environ. Chem. Lett.*, 17, (2019), 1539–1551, doi: 10.1007/s10311-019-00895-9.

[12] J. Guo, S. Khan, S. H. Cho, and J. Kim, "ZnS nanoparticles as new additive for polyethersulfone membrane in humic acid filtration," *J. Ind. Eng. Chem.*, 79 (2019). doi: 10.1016/j.jiec.2019.05.015.

[13] K. Rashid, Q. Alsalhy, A. Figoli, R. Raheem, and F. Al-Ani, "Experimental Investigation of the Effect of Implanting TiO2-NPs on PVC for Long-Term UF Membrane Performance to Treat Refinery Wastewater," *Membranes (Basel).*, 10 (2020) 77.

[14] Q. F. Alsalhy, F. H. Al-Ani, A. E. Al-Najar, and S. I. A. Jabuk, "A study of the effect of embedding ZnO-NPs on PVC membrane performance use in actual hospital wastewater treatment by membrane bioreactor," *Chem. Eng. Process. - Process Intensif.*, 130 (2018) 262-274. doi: 10.1016/j.cep.2018.06.019.

[15] S. Balta, A. Sotto, P. Luis, L. Benea, B. Van der Bruggen, and J. Kim, "A new outlook on membrane enhancement with nanoparticles: The alternative of ZnO," *J. Membr. Sci.*, 389 (2012) 155–161. doi: https://doi.org/10.1016/j.memsci.2011.10.025.

[16] R. J. Kadhim, F. H. Al-Ani, M. Al-shaeli, Q. F. Alsalhy, and A. Figoli, "Removal of Dyes Using Graphene Oxide (GO) Mixed Matrix Membranes," *Membranes* , 10 (2020). doi: 10.3390/membranes10120366.

[17] D. Al-Araji, F. Al-Ani, and Q. Alsalhy, "Modification of polyethersulfone membranes by Polyethyleneimine (PEI) grafted Silica nanoparticles and their application for textile wastewater treatment," *Environ. Technol.*, (2022) 1–17. doi: 10.1080/09593330.2022.2049890.

[18] A. J. Sadiq *et al.*, "Comparative study of embedded functionalised MWCNTs and GO in Ultrafiltration (UF) PVC membrane: interaction mechanisms and performance," *Int. J. Environ. Anal. Chem.*, (2020) 1–22. doi: 10.1080/03067319.2020.1858073.

[19] C. Ursino, R. Castro-Muñoz, E. Drioli, L. Gzara, M. H. Albeirutty, and A. Figoli, "Progress of Nanocomposite Membranes for Water Treatment," *Membranes (Basel).*, 8 (2018) 18. doi: 10.3390/membranes8020018.

[20] E. Demirel, B. Zhang, M. Papakyriakou, S. Xia, and Y. Chen, "Fe2O3 nanocomposite PVC membrane with enhanced properties and separation performance," *J. Membr. Sci.*, 529 (2017) 170-184. doi: 10.1016/j.memsci.2017.01.051.

[21] E. S. Awad, T. M. Sabirova, N. A. Tretyakova, Q. F. Alsalhy, A. Figoli, and I. K. Salih, "A Mini-Review of Enhancing Ultrafiltration Membranes (UF) for Wastewater Treatment: Performance and Stability," *ChemEngineering* , 5 (2021). doi: 10.3390/chemengineering5030034.

[22] M. A. Mohamed *et al.*, "Physicochemical characteristic of regenerated cellulose/N-doped TiO2 nanocomposite membrane fabricated from recycled newspaper with photocatalytic activity under UV and visible light irradiation," *Chem. Eng. J.*, 284 (2016) 202–215. doi: https://doi.org/10.1016/j.cej.2015.08.128.

[23] P. Argurio, E. Fontananova, R. Molinari, and E. Drioli, "Photocatalytic Membranes in Photocatalytic Membrane Reactors," *Processes* , 6 (2018) 162. doi: 10.3390/pr6090162.

[24] N. Li *et al.*, "Self-cleaning PDA/ZIF-67@PP membrane for dye wastewater remediation with peroxymonosulfate and visible light activation," *J. Membr. Sci.*, 591 (2019) 117341. doi: https://doi.org/10.1016/j.memsci.2019.117341.

[25] C. P. Athanasekou *et al.*, "Prototype composite membranes of partially reduced graphene oxide/TiO2 for photocatalytic ultrafiltration water treatment under visible light," *Appl. Catal. B Environ.*, 158–159 (2014) 361–372. doi: https://doi.org/10.1016/j.apcatb.2014.04.012.

[26] X. Zheng, Z.-P. Shen, L. Shi, R. Cheng, and D.-H. Yuan, "Photocatalytic Membrane Reactors (PMRs) in Water Treatment: Configurations and Influencing Factors," *Catalysts* , 7 (2017) 224. doi: 10.3390/catal7080224.

[27] A. Rajeswari, A. Rajeswari, S. Vismaiya, S. Vismaiya, A. Pius, and A. Pius, "Preparation, characterization of nano ZnO-blended cellulose acetate-polyurethane membrane for photocatalytic degradation of dyes from water," *Chem. Eng. J.*, 313 (2017) 928–937. doi: 10.1016/j.cej.2016.10.124.

[28] S. F. Zakeritabar, M. Jahanshahi, M. Peyravi, and J. Akhtari, "Photocatalytic study of nanocomposite membrane modified by CeF3 catalyst for pharmaceutical wastewater treatment," *J. Environ. Heal. Sci. Eng.*, 18 (2020) 1151–1161.

[29] Y. Ishida, S. Motono, W. Doshin, T. Tokunaga, H. Tsukamoto, and T. Yonezawa, "Small Nanosized Oxygen-Deficient Tungsten Oxide Particles: Mechanistic Investigation with Controlled Plasma Generation in Water for Their Preparation," *ACS Omega*, 2 (2017) 5104–5110, doi: 10.1021/acsomega.7b00986.

[30] J. Meng, Q. Lin, T. Chen, X. Wei, J. Li, and Z. Zhang, "Oxygen vacancy regulation on tungsten oxides with specific exposed facets for enhanced visible-light-driven photocatalytic oxidation," *Nanoscale*, 10 (2018) 2908-2915. doi: 10.1039/c7nr08590g.

[31] B. Ma, E. Huang, G. Wu, W. Dai, N. Guan, and L. Li, "Fabrication of WO2.72/RGO nano-composites for enhanced photocatalysis," *RSC Adv.*, 7 (2017) 2606-2614, doi: 10.1039/c6ra26416f.

[32] D. P. Depuccio, P. Botella, B. O'Rourke, and C. C. Landry, "Degradation of methylene blue using porous WO3, SiO2-WO3, and their Au-loaded analogs: Adsorption and photocatalytic studies," *ACS Appl. Mater. Interfaces*, 7 (2015) 1987-1996, doi: 10.1021/am507806a.

[33] M. J. Islam, D. A. Reddy, J. Choi, and T. K. Kim, "Surface oxygen vacancy assisted electron transfer and shuttling for enhanced photocatalytic activity of a Z-scheme CeO2-AgI nanocomposite," *RSC Adv.*, 6 (2016) 19341-19350. doi: 10.1039/c5ra27533d.

[34] M. Weil and W. D. Schubert, "The beautiful colours of tungsten oxides," *ITIA Newsletter*, no. June. 2013.

[35] Z. A. Mohd Hir, A. H. Abdullah, Z. Zainal, and H. N. Lim, "Photoactive Hybrid Film Photocatalyst of Polyethersulfone-ZnO for the Degradation of Methyl Orange Dye: Kinetic Study and Operational Parameters," *Catalysts*, 7 (2017) 313. doi: 10.3390/catal7110313.

[36] G. Frascaroli *et al.*, "Pharmaceuticals in Wastewater Treatment Plants: A Systematic Review on the Substances of Greatest Concern Responsible for the Development of Antimicrobial Resistance," *Applied Sciences* , 11 (2021) 6670. doi: 10.3390/app11156670.

[37] Y. Guo, P. S. Qi, and Y. Z. Liu, "A Review on Advanced Treatment of Pharmaceutical Wastewater," *IOP Conf. Ser. Earth Environ. Sci.*, 63 (2017) 12025. doi: 10.1088/1755-1315/63/1/012025.

[38] C. Gadipelly *et al.*, "Pharmaceutical Industry Wastewater: Review of the Technologies for Water Treatment and Reuse," *Ind. Eng. Chem. Res.*, 53 (2014) 11571–11592, doi: 10.1021/ie501210j.

[39] P. Rabia Tahir, "A Review of Unfractionated Heparin and Its Monitoring," *July 13*, College of Pharmacy and Allied Health Sciences, St. John's University, Jamaica, New York, 2007.

[40] K. B. Johansen and T. Balchen, "Tinzaparin and other low-molecular-weight heparins: what is the evidence for differential dependence on renal clearance?," *Exp. Hematol. Oncol.*, 2 (2013) 21. doi: 10.1186/2162-3619-2-21.

[41] R. R. Abdullah, K. M. Shabeed, A. B. Alzubaydi, and Q. F. Alsalhy, "Novel photocatalytic polyether sulphone ultrafiltration (UF) membrane reinforced with oxygen-deficient Tungsten Oxide (WO2.89) for Congo red dye removal," *Chem. Eng. Res. Des.*, 177 (2022) 526–540. doi: https://doi.org/10.1016/j.cherd.2021.11.015.

[42] S. Wang, W. Fan, Z. Liu, A. Yu, and X. Jiang, "Advances on tungsten oxide based photochromic materials: Strategies to improve their photochromic properties," *Journal of Materials Chemistry C*, 6 (2018) 191-212. doi: 10.1039/c7tc04189f.

[43] Z. X. Low *et al.*, "Enhancement of the Antifouling Properties and Filtration Performance of Poly(ethersulfone) Ultrafiltration Membranes by Incorporation of Nanoporous Titania Nanoparticles," *Ind. Eng. Chem. Res.*, 54 (2015) 11188-11198. doi: 10.1021/acs.iecr.5b03147.

[44] L. A. Shah, T. Malik, M. Siddiq, A. Haleem, M. Sayed, and A. Naeem, "TiO2 nanotubes doped poly(vinylidene fluoride) polymer membranes (PVDF/TNT) for efficient photocatalytic degradation of brilliant green dye," *J. Environ. Chem. Eng.*, 7 (2019) 103291. doi: 10.1016/j.jece.2019.103291.

[45] A. L. Ahmad, J. Sugumaran, and N. F. Shoparwe, "Antifouling properties of PES membranes by blending with ZnO nanoparticles and NMP-acetone mixture as solvent," *Membranes (Basel).*, 8 (2018) 131. doi: 10.3390/membranes8040131.

[46] M. Algamdi, I. Alsohaimi, J. Lawler, H. Ali, A. Aldawsari, and H. Hassan, "Fabrication of Graphene Oxide incorporated Polyethersulfone Hybrid Ultrafiltration Membranes for Humic Acid Removal," *Sep. Purif. Technol.*, 223 (2019) 17-23. doi: 10.1016/j.seppur.2019.04.057.

[47] V. Vatanpour *et al.*, "Anti-fouling polyethersulfone nanofiltration membranes aided by amine-functionalized boron nitride nanosheets with improved separation performance," *J. Environ. Chem. Eng.*, 8 (2020) 104454. doi: 10.1016/j.jece.2020.104454.

[48] Y. Gao, M. Hu, and B. Mi, "Membrane surface modification with TiO2–graphene oxide for enhanced photocatalytic performance," *J. Memb. Sci.*, 455 (2014) 349–356. doi: https://doi.org/10.1016/j.memsci.2014.01.011.

[49] D. Liu *et al.*, "WO3−x for rapid adsorption and full-spectrum-responsive photocatalytic activities," *J. Mater. Sci. Mater. Electron.*, 29 (2018) 15029–15033. doi: 10.1007/s10854-018-9641-8.

[50] D. Shinde, P. Tambade, M. Chaskar, and K. Gadave, "Photocatalytic degradation of Dyes in Water by Analytical Reagent Grade Photocatalysts – A comparative study," *Drink. Water Eng. Sci. Discuss.*, 10 (2017) 109-117. doi: 10.5194/dwes-2017-20.

[51] S. Ren, C. Boo, N. Guo, S. Wang, M. Elimelech, and Y. Wang, "Photocatalytic Reactive Ultrafiltration Membrane for Removal of Antibiotic Resistant Bacteria and Antibiotic Resistance Genes from Wastewater Effluent," *Environ. Sci. Technol.*, 52 (2018) 8666–8673. doi: 10.1021/acs.est.8b01888.

[52] S. F. Zakeritabar, M. Jahanshahi, and M. Peyravi, "Photocatalytic Behavior of Induced Membrane by ZrO2_SnO2 Nanocomposite for Pharmaceutical Wastewater Treatment," *Catal. Letters*, 148 (2018) 882–893.

[53] H. Karimipour, A. Shahbazi, and V. Vatanpour, "Fabrication and characterization of a high-flux and antifouling polyethersulfone membrane for dye removal by embedding Fe3O4-MDA nanoparticles," *Chem. Eng. Res. Des.*, 145 (2019) 64-75. doi: 10.1016/j.cherd.2019.03.003.

[54] Z. Xu *et al.*, "Photocatalytic antifouling PVDF ultrafiltration membranes based on synergy of graphene oxide and TiO2 for water treatment," *J. Memb. Sci.*, 520 (2016) 281-293. doi: 10.1016/j.memsci.2016.07.060.